JOURNAL OF APPLIED ELECTROCHEMISTRY 22 (1992) 262–267

X-ray diffraction study of anisotropy by formation and decomposition of nickel hydride Part I: Orientation dependence of the extent of phase transformation of nickel into nickel hydride

I. TOMOV, M. MONEV

Institute of Physical Chemistry, Bulgarian Academy of Sciences, 1040 Sofia, Bulgaria

Received 16 October 1990; revised 14 April 1991

The effect of microstructure and crystal direction on the extent of phase transformation (EPT) of Ni into β-NiH by cathodic charging with H has been investigated by X-ray diffraction. A measure for EPT in each crystal direction is the relevant volume fraction of β-NiH. EPT is controlled by the crystal direction in the case of heat-treated specimens. In the case of electrodeposited specimens, the imperfections of which are commensurate with those of cold-worked metals, EPT is controlled by both the crystal direction and the "dislocation-induced" anisotropy at the same time. The study provides new information on the characteristics of the phase transformation of bulk nickel into β-NiH.

1. Introduction

It is well known that as a result of cathodic charging with H (both of electrodeposited layers and metallurgically produced nickel) in the presence of inhibitors, a nickel hydride phase is produced which is unstable at room temperature [1–6]. This phase, denoted as β-NiH, coexists alongside α-Ni [6]. α-Ni is a solid solution of about 5 at. % H in nickel. Above this mean content, there is an abrupt formation of β-NiH, the H : Ni ratio of which is 0.7–0.8. α-Ni and β-NiH possess a FCC lattice: the lattice constant of β-NiH is 0.3738 nm – it is about 6% greater than the lattice constant of nickel, which is 0.3524 nm [1, 6]. β-NiH, formed during the cathodic charging with H in the surface layer of the textured electrodeposited nickel, has the same crystallite orientation as the nickel matrix [7].

The X-ray diffraction (XRD) measurements of β-NiH are relative, since the comparison with standards is not possible [5, 8, 9]. Such an approach was employed to monitor the influence of the electrochemical conditions of cathodic charging with H on the decomposition kinetics of β-NiH. A model for the role of dislocations in the formation and decomposition has been proposed on the basis of the differences in the decomposition rates of β-NiH formed as a result of the cathodic charging with H in the presence and absence of Cu^{2+} [6, 9, 10]. Thus the influence of one of the structure parameters on the phase transformation is accounted for in practice. In a previous study [11], it was established that the extent of phase transition of nickel into β-NiH is greater in bright coatings than in matt ones. This indicates that the observed difference may be due to both a difference in their texture and microstructure. The existence of such a difference for analogous coatings has been established in [12]. If a property is dependent on the structure, it should then be an anisotropic property, since "the structure anisotropy is a source of anisotropy of the properties" [13]. It is known that the diffusion rate is to a great degree dependent on the crystallographic direction [14]. The diffusion of the H atoms to the sites of their trapping (sites of the elementary act of phase transformation) is carried out through the grain and twin boundaries, crystal lattice and its defects. Thus the question arises whether the extent of phase transformation of nickel into β-NiH depends (and eventually how does it depend?) on the Ni crystallite orientation and microstructure anisotropy (differing size and microdeformation of the crystallites in the different crystal directions). This study is a first attempt to find an answer to this question.

2. Specimen preparation and experimental details

Most of the models for this study were nickel coatings, deposited on 1 × 25 × 35 mm copper substrates. In an XRD sense, the 50 μm thick coatings behaved as bulk metal, since their thickness was greater than the effective depth of X-ray penetration [15]. The electrodeposition conditions (listed in Table 1) were selected in such a way as to obtain coatings with differing microstructure and texture. To this end matt, half-bright, and bright coatings with different surface morphologies were prepared [12]. The nickel layers were not detached from their substrates. The rest of the models were 1 mm × 25 mm × 35 mm plates of commercial high-purity (99.5% and 99.7%) nickel. All specimens given in the table are representative of 3 or 4 other specimens.

The cathodic charging of Ni with H was carried out

0021-891X/92

Table 1. Electrolytes and conditions for deposition of nickel coatings. Main composition: $NiSO_4 \cdot 7H_2O$ – 280 g dm^{-3}, H_3BO_3 – 30 g dm^{-3}, pH 4.5.

No.	$NiCl_2 \cdot 6H_2O$ g dm^{-3}	Additives (g dm^{-3})		Temperature (° C)	Current density (A dm^{-2})	Surface type
		Saccharin	Butyndiol			
1	–	–	–	50	5	matt
2	50		–	18	3	matt
3	50	–	0.05	50	5	matt
4	–	–	–	18	5	matt
5	50	1.0	0.025	50	5	half-bright
6	50	1.0	0.20	50	5	bright

at room temperature in an electrolysis bath consisting of: 1 N H_2SO_4 and H_2SeO_3 at 10 mg dm^{-3}. The duration of cathodic charging was 30 min at a current density of $D_k = 1$ A dm^{-2}. Specimens were charged in the as-fabricated state as well as in the heat treated state. The annealed nickel coatings and plates were H-charged after electrolytic polishing. The polishing was carried out in a 60% H_2SO_4 aqueous solution at about 35° C and 40 A dm^{-2} for 20 s.

3. Experimental methods

The quantitative expression of the β-NiH phase as a result of XRD measurements was carried out by directly comparing the integrated intensities $I_{i(\beta\text{-NiH})}$ and $I_{i(\alpha\text{-Ni})}$ which diffracted in directions with the same i-indices of the two phases, respectively

$$f_i = \frac{I_{i(\beta\text{-NiH})}}{I_{i(\beta\text{-NiH})} + I_{i(\alpha\text{-Ni})}} \tag{1}$$

where the volume fraction f_i of β-NiH is the ratio of the volume of i-oriented β-NiH crystallites to the volume of all i-oriented crystallites in the two-phase system. Since the i-oriented β-NiH crystallites are formed of i-oriented nickel crystallites [7], f_i accounts for the phase transformation of only crystallites with ideal i-orientation, i.e. f_i is a measure of the extent of phase transformation (EPT) of nickel in the respective i-crystal direction.

There are two reasons which determine the use of the above simplified expression (Equation 1):

1. the orientation distribution of the two phases is analogous, since the "growth" of the β-NiH crystallites during H-charging is a result of the isotropic increase of the parameter of α-Ni crystallites, as follows from [7], and
2. the theoretical integrated intensities, calculated with the respective equation [17], for a series of diffraction lines of the two phases with the same indices, differ by less than 2%. This series contains the 1 1 1, 2 0 0, 2 2 0 and 3 1 1 lines. In an earlier study Equation 1 was applied only to the 1 1 1 diffraction line of the two phases [11].

The apparent crystal (or coherent domain) size D_i and the microdeformation e_i were determined by the single line method [18, 19].

$$D_i = \frac{\lambda}{\beta_C^f \cos\theta} \tag{2}$$

$$e_i = \frac{\beta_G^f}{4 \tan\theta} \tag{3}$$

where λ is the wavelength, θ is the Bragg angle, β_C^f and β_G^f are the Cauchy (C) and Gaussian (G) components of the integral breadths of the pure diffraction profile (f), respectively.

The measurements of the 1 1 1, 2 0 0, 2 2 0 and 3 1 1 diffraction lines of β-NiH and α-Ni were performed with an X-ray diffractometer Philips with CuK_α radiation (LiF focusing monochromator). The measurements gave information on the structure in the ⟨1 1 1⟩, ⟨1 0 0⟩, ⟨1 1 0⟩ and ⟨3 1 1⟩ directions, respectively. The apparent size and the microdeformations of the crystallites in the same directions were determined prior to the cathodic H-charging. To this end CoK_β radiation isolated with the help of a LiF focusing monochromator was used.

The study was carried out at room temperature. The time for measuring the integrated intensity (area) for each line was 100 s, i.e. it is negligible compared to the experimentally established time of decomposition of β-NiH.

4. Results and discussion

4.1. *Texture of specimens*

The electrodeposited nickel coatings have a fibre texture. The specimen texture was determined from the pole figures, measured with a texture goniometer. The growth textures of the different specimens had the following ⟨u v w⟩ components: ⟨1 0 0⟩ + ⟨2 2 1⟩; ⟨1 1 0⟩ + ⟨4 1 1⟩; ⟨1 1 1⟩ + ⟨1 0 0⟩; ⟨2 1 0⟩ + ⟨5 4 2⟩ and ⟨2 1 1⟩ + ⟨7 2 1⟩ (see Table 2). The high-indexed directions correspond to twin components of the first order [16]. The method for determining the twin orientation of the first and second order, arising in different matrix orientations (main components) is given in [16], Figs 1–3 show pole figures which illustrate the presence of twin components ⟨4 1 1⟩, ⟨5 4 2⟩ and ⟨7 2 1⟩, respectively. The commercial nickel plates showed a sheet texture with a predominance of the ⟨1 0 0⟩ component.

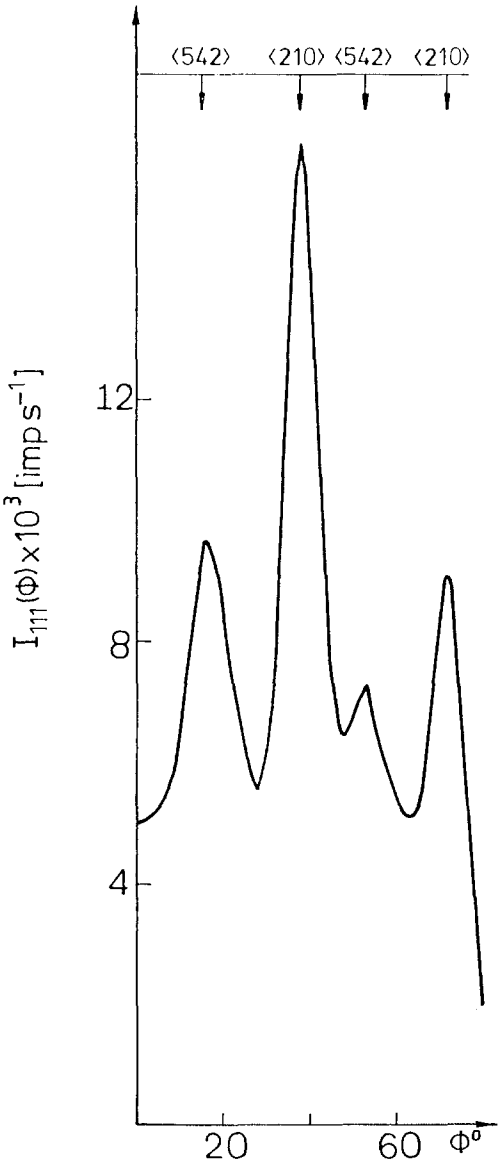

Fig. 1. $I_{111}(\Phi)$ – pole figure of an electrolytically deposited nickel layer (specimen 2) acording to Table 2. Φ° – angle to the layer normal direction. Main texture component ⟨2 1 0⟩ with angle position of the maxima 39.23° and 75.04°. Twin texture component ⟨5 4 2⟩ with angle position of the maximums 18.79° and 52.95°.

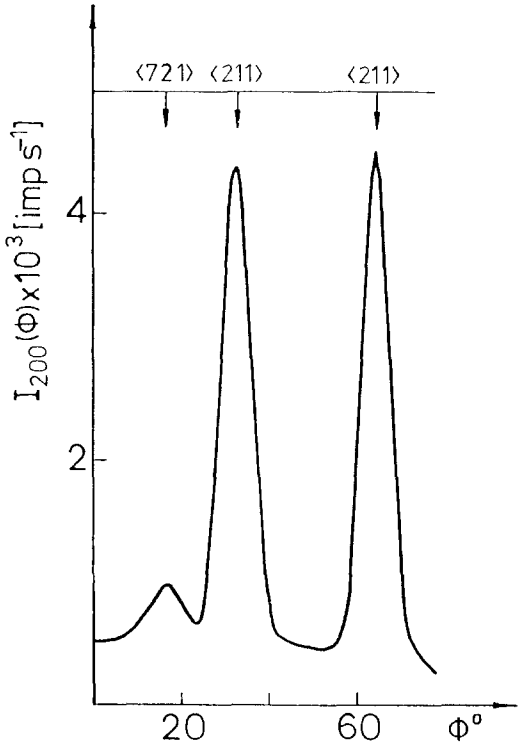

Fig. 2. $I_{200}(\Phi)$ – pole figure of an electrolytically deposited nickel layer (specimen 3) according to Table 2. Φ° – angle to the layer normal direction. Main texture component ⟨2 1 1⟩ with angle position of the maxima 35.26° and 65.91°. Twin component first order ⟨7 2 1⟩ with angle position of the maximum 17.72°.

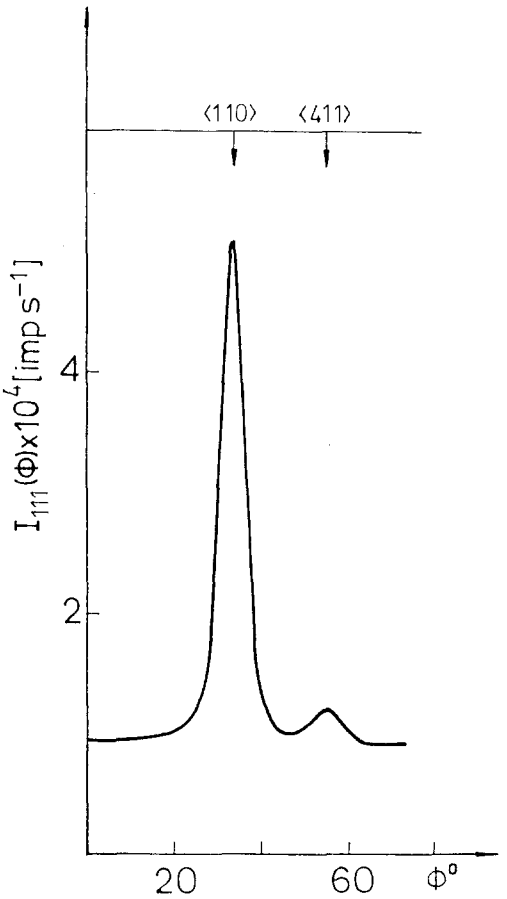

Fig. 3. $I_{111}(\Phi)$ – pole figure of an electrolytically deposited nickel layer (specimen 4) according to Table 2. Φ° – angle to the layer normal direction. Main texture component ⟨1 1 0⟩ with angle position of the maximum 35.26°. Twin component first order ⟨4 1 1⟩ with angle position of the maximum 57.02°.

4.2. *EPT of nickel into nickel hydride*

To establish the way the structure parameters influence EPT, f_i was determined in specimens H-charged both in their after as-fabricated state and after their heat treatment. For the specimens H-charged in their as-fabricated state, the f_i vaues should be dependent both on the crystallite orientation and the microstructure anisotropy (differing size and microdeformations of the crystallites in the different *i*-crystal directions).

If the f_i values are equal in all *i*-directions of a given specimen, then there is a case of homogeneous phase transformation. In reality, however, the f_i data given in Table 2 indicate that the phase transformation has occurred to a different degree in the ⟨1 1 1⟩, ⟨1 0 0⟩, ⟨1 1 0⟩, ⟨3 1 1⟩ directions in all specimens, i.e. there is an anisotropy of EPT of nickel into β-NiH. Evidently f_i is considerably greater in the ⟨1 1 1⟩ and ⟨1 0 0⟩

Table 2. Volume fractions f_i of nickel hydride (β-NiH) in some ⟨h k l⟩ crystal directions of nickel coatings cathodically charged with hydrogen in the as-fabricated state. Δf – error due to counting statistics. ⟨u v w⟩ – indices of growth texture.

No.	⟨u v w⟩	$f_i + \Delta f$				Surface type
		⟨1 1 1⟩	⟨1 0 0⟩	⟨1 1 0⟩	⟨3 1 1⟩	
1	1 0 0 + 2 2 1	0.49 ± 0.004	0.44 ± 0.001		0.27 ± 0.007	matt
2	2 1 0 + 5 4 2	0.56 ± 0.005	0.67 ± 0.005	0.30 ± 0.007	0.35 ± 0.007	matt
3	2 1 1 + 7 2 1	0.57 ± 0.004	0.54 ± 0.008		0.39 ± 0.004	matt
4	1 1 0 + 4 1 1	0.49 ± 0.005	0.38 ± 0.008	0.07 ± 0.0005	0.17 ± 0.007	matt
5	1 0 0 + 2 2 1	0.69 ± 0.003	0.73 ± 0.002		0.45 ± 0.006	half-bright
6	1 1 1 + 1 0 0	0.78 ± 0.003	0.76 ± 0.004		0.51 ± 0.006	bright

directions than in the ⟨3 1 1⟩ and ⟨1 1 0⟩ directions*. There are two clearly manifest trends of this non-homogeneous phase transformation. The EPT anisotropy of the bright and matt nickel layers (not counting among the latter specimen No. 2 with a ⟨2 1 0⟩ texture) can be represented generally by the inequalities:

$$f_{111} > f_{100} > f_{311} > f_{110} \tag{4}$$

while for the half-bright and matt (with a ⟨2 1 0⟩ main texture component) nickel coatings the following inequalities are valid

$$f_{100} > f_{111} > f_{311} > f_{110} \tag{5}$$

The circumstance that the anisotropy of the pahse transformation is described by two inequalities (4 and 5) suggests that EPT depends both on the crystal direction and the microstructure anisotropy. The main problem is how to distinguish the influence of the different structure parameters on EPT. This requires the next step of the study to be linked to obtaining information on the apparent crystal size and microdeformations.

4.3. *Effect of microstructure anisotropy on EPT*

The microstructure parameters were determined prior to charging with H. Table 3 lists the values of the apparent crystal size D_i (upper lines) and microdeformations e_i (lower lines). D_i of all matt coatings (specimens no.'s 1–4) in all crystal directions are considerably greater than the D_i of the bright coatings (specimen No. 6). Moreover these results indicate that D_i is anisotropic. A specific characteristic of the crystalline size anisotropy is that D_i is largest in the direction of the main texture component [20]. This is also confirmed in this case: the apparent crystal size is greatest in the ⟨1 0 0⟩, ⟨1 1 0⟩, ⟨1 0 0⟩ and ⟨1 1 1⟩ for specimens no.'s 1, 4, 5, 6, respectively†.

The results indicate the specificity of the crystal size anisotropy for each concrete growth texture, and that it does not correlate with the anisotropy of phase transformation as expressed by the two series of inequalities (4) and (5). What is more, the hydrogen, diffusing along the grain and twin boundaries can aid the phase transformation in the crystallites, irrespectively of their orientation. But since the diffusion proceeds with a greater rate along the grain and twin boundaries (the area of which depends on the mean crystallite size), than through the crystal interior [21], the grain and twin boundaries favour the phase transformation by facilitating the supply of H to the bulk of the specimen. This is confirmed by the experimental fact that in specimen No. 6, with the least mean crystallite size (and consequently with the largest area of grain and twin boundaries), EPT is greatest, compared to that of the other specimens. It is also evident that EPT falls continuously with increase in D_i, i.e. from bright through half-bright to matt coatings (compare Table 2 with Table 3).

Earlier papers [6, 9, 10] discuss the role of dislocations in β-NiH formation. On the basis of the experimental results an assessment of the role of microdeformations on the EPT is attempted. By origin they are linked mainly with the tension fields around dislocations in the crystal interior [22], which is the reason why the microdeformations may be used as a

Table 3. Apparent crystallite (or coherent domain) size D_i (upper lines) and microdeformations e_i (lower lines) in some ⟨h k l⟩ directions before cathodically charging with hydrogen of the nickel electrodeposited layers. XRD measurements with CoK_β-radiation. LiF focusing monochromator.

No.	$D_i \pm \Delta D$ (nm) – upper line $(e_i \pm \Delta e) \times 10^3$ – lower line			
	⟨1 1 1⟩	⟨1 0 0⟩	⟨1 1 0⟩	⟨3 1 1⟩
1	91 ± 7 1.5 ± 0.2	> 150 1.5 ± 0.1		59 ± 6 1.3 ± 0.1
2	87 ± 6 2.8 ± 0.2	56 ± 4 4.1 ± 0.2		23 ± 2 1.5 ± 0.2
3	45 ± 3 1.5 ± 0.2	38 ± 4 3.5 ± 0.4		52 ± 6 2.2 ± 0.2
4	49 ± 6 1.5 ± 0.2	44 ± 7 1.5 ± 0.2	96 ± 8 2 ± 0.2	40 ± 5 1.7 ± 0.2
5	32 ± 4 3.6 ± 0.3	94 ± 8 5.1 ± 0.4		22 ± 5 3.3 ± 0.3
6	28 ± 4 4.1 ± 0.2	17 ± 2 7.9 ± 0.6		19 ± 3 5.4 ± 0.4

* Because of the presence of a texture it was not possible to measure the 220 lines of α-Ni and β-NiH in all cases, which is the reason for the limited number of f_{110} determinations.

† It was impossible to measure the apparent crystal size D_i in the ⟨2 1 0⟩ and ⟨2 1 1⟩ directions with CoK_β-radiation because of technical considerations.

Table 4. Volume fractions f_i of nickel hydride (β-NiH) in some ⟨h k l⟩ crystal directions of nickel coatings cathodically charged with hydrogen and flat-plate commercial nickel of high purity after heat treatment. Δf — error due to counting statistics. ⟨u v w⟩ — indices of recrystallization texture.

No.	⟨u v w⟩	$f_i + \Delta f$				Surface type
		⟨111⟩	⟨100⟩	⟨110⟩	⟨311⟩	
1′	100 + 221	0.51 ± 0.003	0.18 ± 0.001		0.15 ± 0.006	matt
2′	100 + 110 + 210	0.50 ± 0.004	0.35 ± 0.002	0.15 ± 0.005	0.18 ± 0.006	matt
3′	100 + 221	0.54 ± 0.003	0.24 ± 0.002		0.14 ± 0.006	matt
4′	100 + 210 + 110	0.39 ± 0.004	0.15 ± 0.002	0.04 ± 0.001	0.09 ± 0.007	matt
5′	100 + 221	0.38 ± 0.004	0.24 ± 0.001		0.18 ± 0.005	half-bright
6′	100 + 111	0.51 ± 0.004	0.24 ± 0.002	0.11 ± 0.005	0.18 ± 0.008	bright
7′	100	0.51 ± 0.003	0.21 ± 0.002	0.09 ± 0.003	0.11 ± 0.005	99.5% purity
8′	100	0.45 ± 0.003	0.31 ± 0.001	0.11 ± 0.002	0.15 ± 0.004	99.7% purity

measure for assessing the dislocation density [23]. The dislocation density in electrodeposited metals [24, 25] is commensurate with that of cold-worked metals, for which it is 10^{11} to 10^{12} dislocations per cm^2 [26]. The values obtained for the dislocation density from D_i and e_i data (see Table 3), on the basis of [23], are within the limits 8×10^{10} to 2×10^{12} dislocations per cm^2. The highest dislocation density was established for bright coatings (specimen No. 6), and the lowest — for matt coatings (specimen No. 1). Because of the existing analytical connection between the microdeformations and dislocation density [23], the two terms will be used interchangeably.

The microdeformation values increase in the order from matt to bright coatings. Within the set of matt coatings this order depends in addition on the texture. The e_i distribution has an anisotropic character. Thus for most of the specimens the results reveal a trend for relatively higher microdeformations in the ⟨1 0 0⟩ direction compared to the other crystal directions. This trend is especially clearly expressed for specimens No.'s 2, 5, 6 (Table 3) for which e_i are very high. In fact, inequalities (5) are valid for specimens No.'s 2 and 5, i.e. the characteristic for most of the order of EPT of nickel into β-NiH (Inequalities 4) is changed by the fulfillment of $f_{100} > f_{111}$, while for specimen No. 6 f_{100} becomes almost equal to f_{111}. These facts undoubtedly confirm that the dislocation-induced anisotropy causes anisotropy of EPT and that the dislocations strongly favour the phase transformation of nickel into β-NiH. They are in agreement with the assumption proposed in [27, 28] that the dislocations act as H traps and thus support the model for the role of the dislocations for the formation of β-NiH [6, 9, 10].

The question arises as to what changes occur with anisotropy of phase transformation, if the dislocation-induced anisotropy is eliminated. This determined the next step in the study; to investigate the influence of the crystal structure obtained as a result of annealing processes (recovery, recrystallization, grain growth) on the EPT of nickel into β-NiH.

4.4. *EPT of Ni into β-NiH in thermally treated specimens*

The thermal treatment of the above specimens was carried out at 520° C in an argon atmosphere (purified of oxygen) for 5 h. The data on the recrystallization texture obtained from the analysis of the pole figures are presented in Table 4, column ⟨u v w⟩. In fact, the specimens now possess a new structure, and this is reflected in their notation by the addition of a ′-mark. In all cases the ⟨1 0 0⟩ recrystallization component was observed, but for specimens Nos. 2, 4 the ⟨1 1 0⟩ and ⟨2 1 0⟩ main components of recrystallization texture, respectively were also observed. As a result of the recrystallization some crystallites had grown considerably, the consequence of which was that they had their own detectable reflections on the pole figures. The structure of the annealed plates of commercial nickel was analogous — the size of their crystallites was of the order of a few microns, which also followed from their pole figures. According to [29] the annealed metals contain 10^6 to 10^8 dislocations per cm^2, which means that the dislocation density of our specimens is 3–4 orders of magnitude lower than that of their non-annealed state. This determines a reduced permeation of H in nickel crystallites as has been discussed for an analogous case in [30]. As a rule the annealing process leads to the onset of a similarity in the texture, crystal size and dislocation density. This similarity reflects on a decrease in f_i common for all specimens compared to its values for the nonannealed state. The sharp decrease in f_{100} for specimens Nos. 2, 5, 6 which, in some cases, is 2–3 times less than f_{100} for the nonannealed state of the same specimens is evident. By means of the experiments with annealed specimens, for which the transport of H toward the interior is hindered because of the lowered dislocation density and diminished grain and twin boundaries area (because of the increased crystallite size), the promoting role of these two structure parameters on EPT is again revealed.

The EPT anisotropy in the investigated crystal direc-

tions is described by the inequalities (4) for all thermally treated specimens. What is more, the ratio of f_{111} and f_{100} for most of the specimens can be expressed approximately by the factor 2 (see Table 4). Therefore after annealing, that is after eliminating the influence of the dislocation-induced anisotropy, it becomes evident that the main factor which affects EPT is the crystallographic direction. This is one of the most important results of the study.

A careful examination of the data in Table 4 indicates that in the case of annealed nickel, after cathodic charging with H, the f_i values in crystallographically equivalent directions of all specimens differ. The f_i ratios in the crystallographically non-equivalent directions also differ for all specimens. A possible reason for the absence of constant f_i ratios may be the presence, as well as the distribution, of impurities in the nickel. In the case of electrodeposited coatings the impurities come from the electrolytic bath. It is known, however, that the impurities, acting as H-traps, may be factors affecting the phase transformation [31, 32].

5. Conclusion

The phase transformation of nickel into β-NiH is anisotropic. The present studies indicate that the anisotropy of EPT in polycrystals, consisting of crystallites with lattice imperfections, is controlled by two factors:

(i) crystallographic direction, i.e. orientation of the crystallites versus surface of charging with H.
(ii) "dislocation induced" anisotropy, i.e. the orientation distribution of dislocation density.

In the case of polycrystals, consisting of "perfect" crystallites which have grown during the annealing process, the anisotropy of the phase transformation is controlled by one main factor – the crystallographic direction.

The discussion so far indicates that the mean EPT value should depend not only on the above parameters, but also on the texture (through the distribution of the occurring crystal directions) and on the mean crystallite size (through the area of the grain and twin boundaries).

The different EPT observed in the different crystal directions is, in essence, an indication of the occurrence of an orientation dependent process during the charging of Ni with H. The orientation dependence of EPT of nickel into β-NiH is undoubtedly a consequence of the differing rates of permeability of H in the relevant crystal directions of a nickel polycrystal.

Acknowledgement

The authors would like to thank T. Bozhinova, a technical assistant in the X-Ray Diffraction Laboratory of the Institute of Physical Chemistry at the Bulgarian Academy of Sciences, for the measurements.

References

[1] A. Janko, *Naturwiss.* **47** (1960) 225.
[2] T. Boniszewski and G. C. Smith, *J. Phys. Chem. Solids* **21** (1961) 115.
[3] B. Baranowski, *Roczniki Chemii Ann. Soc. Chim. Polon.* **38** (1964) 1019.
[4] I. W. Calbe, E. O. Wollan and W. H. Kocher, *Le J. de Phys.* **25** (1964) 460.
[5] P. Ch. Borbe, F. Erdmann-Jesnitzer and W. Schoebel, *Z. Metallkunde* **71** (1980) 227.
[6] J. Pielaszek, in 'Hydrogen Degradation of Ferrous Alloys' (edited by R. A. Oriani, J. P. Hirth and M. Smialowski), New Public. Park Ridge, USA (1985) p. 167.
[7] S. Majchrzak and H. Jarmolowicz, *Bull. Acad. Polon. Sci. (ser. sci. chim.)* **12** (1964) 155.
[8] A. Janko, *ibid.* **10** (1962) 617.
[9] J. Pielaszek, *ibid.* **20** (1972) 611.
[10] J. Pielaszek, *ibid.* **20** (1972) 484.
[11] St. Rashkov, M. Monev and I. Tomov, *Surf. Technol.* **16** (1982) 203.
[12] St. Vitkova, I. Tomov and V. Velinov, *Bulg. Acad. Sci. (commun. depart. chem.)* **11** (1978) 258.
[13] H. J. Bunge, in 'Directional Properties of Materials' (edited by H. J. Bunge), DGM Informationsgeselschaft-Verlag, Oberursel (1988) p. 1.
[14] K. Meyer, Physikalisch-Chemische Krystallographie, VEB Deutscher Verlag für Grundstoffindustrie, Leipzig (1968) (russian transl. p. 243).
[15] I. Tomov, *Phys. Stat. Sol. (a)* **95** (1986) 397; **98** (1986) 43.
[16] I. Tomov, *Bulg. Acad. Sci. (commun. depart. chem.)* **9** (1976) 192.
[17] B. D. Cullity, 'Elements of X-Ray Diffraction', Addison-Wesley, London (1967) p. 269.
[18] J. I. Langford, *J. Appl. Cryst.* **11** (1978) 10.
[19] R. Delhez, Th. H. de Kaijser and E. J. Mittemeijer, *Fres. Z. Anal. Chem.* **112** (1982) 1.
[20] Sv. Surnev and I. Tomov, *J. Appl. Electrochem.* **19** (1989) 75.
[21] J. C. Fisher, *J. Appl. Phys.* **22** (1950) 74.
[22] M. B. Bever, D. L. Holt and A. I. Titchner, in 'Progress in Materials Science', Vol. 17 (edited by B. Chalmers, J. W. Christian and T. B. Massalski), Pergamon Press, Oxford (1973).
[23] G. K. Williamson and R. E. Smollman, *Phil. Mag.* **1** (1956) 34.
[24] R. W. Hinton, L. H. Schwartz and J. B. Cohen, *J. Electrochem. Soc.* **110** (1963) 103.
[25] E. M. Hofer and H. E. Hintermann, *ibid.* **112** (1965) 167.
[26] W. T. Read and W. Shockley, 'Imperfections in Nearly Perfect Crystals', Wiley & Sons, New York (1952) p. 166.
[27] A. Atrens, D. Mezzanote, N. F. Fiore and A. Genshaw, *Corros. Sci.* **20** (1980) 673.
[28] R. M. Latanision and M. Kurkela, *Corrosion-Nice* **39** (1983) 174.
[29] P. B. Hirsch, *Progr. Metal Phys.* **6** (1956) 236.
[30] W. Paatsch, *Plat. and Surf. Fin.* **75** (1988) 52.
[31] J. W. Larsen and B. R. Livesay, *J. Less-Common Metals* **73** (1980) 79.
[32] I. G. Douglas and D. O. Northwood, *J. Mater. Sci.* **18** (1983) 321.